The American Journal of Pathology, Vol. 173, No. 3, September 2008
Copyright © American Society for Investigative Pathology
DOI: 10.2353/ajpath.2008.080006

Tumorigenesis and Neoplastic Progression

Soluble Forms of the Notch Ligands Delta1 and Jagged1 Promote *in Vivo* Tumorigenicity in NIH3T3 Fibroblasts with Distinct Phenotypes

Sumithra Urs,* Alice Roudabush,† Christine F. O'Neill,‡ Ilka Pinz,* Igor Prudovsky,* Doreen Kacer,* Yuefang Tang,* Lucy Liaw,* and Deena Small§

From the Center for Molecular Medicine, Maine Medical Center Research Institute, Scarborough, Maine; Department of Animal and Nutritional Sciences and New Hampshire Veterinary Diagnostics Laboratory,† University of New Hampshire, Durham, New Hampshire; Department of Biochemistry,‡ Boston University, Boston Massachusetts; and Department of Biochemistry and Molecular Biology,§ University of New Hampshire, Durham, New Hampshire*

We previously found that soluble forms of the Notch ligands Jagged1 and Delta1 induced fibroblast growth factor receptor-dependent cell transformation in NIH3T3 fibroblasts. However, the phenotypes of these lines differed, indicating distinct functional differences among these Notch ligands. In the present study, we used allografts to test the hypothesis that NIH3T3 fibroblasts that express soluble forms of Delta1 and Jagged1 accelerate tumorigenicity *in vivo*. With the exception of the full-length Jagged1 transfectant, all other cell lines, including the control, generated tumors when injected subcutaneously in athymic mice. Suppression of Notch signaling by the soluble ligands significantly increased tumor onset and growth, whereas full-length Jagged1 completely suppressed tumor development. In addition, there were striking differences in tumor pathology with respect to growth kinetics, vascularization, collagen content, size and number of necrotic foci, and invasiveness into the underlying tissue. Further, the production of angiogenic factors, including vascular endothelial growth factor, also differed among the tumor types. Lastly, both Jagged1- and Delta1-derived tumors contained phenotypically distinct populations of lipid-filled cells that corresponded with increased expression of adipocyte markers. The divergence of tumor phenotype may be attributed to ligand-specific alterations in Notch receptor responses in exogenous and endogenous cell populations within the allographs. Our findings demonstrate distinct functional properties for these Notch ligands in the promotion of tumorigenicity *in vivo*. *(Am J Pathol 2008, 173:865–878; DOI: 10.2353/ajpath.2008.080006)*

The Notch signaling system is an evolutionarily conserved pathway that regulates cell fate decisions including quiescence, proliferation, differentiation, and death.[1–3] Four receptors (Notch1–Notch4) and eight putative ligands (Jagged1–Jagged2, Delta1–Delta4, F3/contactin, Pref-1) have been identified in vertebrates to-date and despite structural similarity and overlapping patterns of expression, the Notch receptors and ligands are not functionally redundant as null mutations for each display unique phenotypes.[4–14] The identity of the activating ligand has also been demonstrated to influence the outcome of Notch signaling events in cell culture systems and *in vivo*, indicating that regulation of specific receptor/ligand interactions is important for defining the Notch-mediated response.[15–17]

In the classic model of Notch signaling, ligand binding results in the proteolytic processing of the Notch receptor and subsequent release of the intracellular domain from the remainder of the protein.[18–20] The Notch intracellular domain then translocates into the nucleus where it interacts with the CSL family of transcription factors, turning them from repressors to activators of transcription.[21–23] Notch targets include genes encoding the HES and HEY/HRT transcription factor families,[24,25] which, in turn, alter the expression of master regulatory factors such as MASH and MyoD.[24,26] A non-canonical Notch signaling pathway mediated by the cytoplasmic protein Deltex is

Supported by NIH grants NRCSA-CA92255 (D.S.), R15DK070599 (D.S.), R01HL070865 (L.L); and grant P20RR15555 (R.E.F., L.L.) from the National Center for Research Resources. This is Scientific Contribution Number 2364 from the New Hampshire Agricultural Experiment Station.

L.L. and D.S. contributed equally to this work.

Accepted for publication June 16, 2008.

Address reprint requests to Deena J. Small, Ph.D., Department of Biochemistry, 389 Rudman Hall, University of New Hampshire, Durham, New Hampshire 03824. E-mail: dsmall@.unh.edu.

also thought to occur, although this Notch-mediated signaling mode is less characterized.[27,28] The intracellular domains of at least two of the ligands (Delta1 and Jagged1) also contain nuclear localization signals that permit their entry into the nucleus, although their direct role(s) in regulating nuclear functions are unclear.[29–31]

We and others have previously demonstrated that non-transmembrane, soluble forms of the Delta1 and Jagged1 ligands repress Notch activation, possibly by acting as competitors for binding of the full-length, endogenous ligands to the Notch receptors.[32,33] Using the NIH3T3 cell, a standard cell transformation model, we found that expression of these soluble forms of Jagged1 (sJag1) and Delta1 (sDl1) induced fibroblast growth factor receptor (FGFR)-dependent transformation *in vitro*.[16,33] Interestingly, the phenotype of cells stably expressing these two different ligands were distinct in their regulation of cell-cell adhesion, the actin cytoskeleton, and cell migration.[16] Given the divergent activities of Notch signaling in cell transformation versus tumor suppression in different tissues,[34] our present study tests the *in vivo* tumorigenic phenotype of NIH3T3 cells expressing either full-length ligands or dominant negative, soluble ligand forms. Our studies validate that Notch signaling through Jagged1 is a potent inhibitor of *in vivo* tumorigenesis in this model, whereas expression of Delta1 did not impede overall tumor growth. Conversely, inhibition of endogenous Notch/ligand interactions through expression of either sDl1 or sJag1 promotes tumorigenicity of the NIH3T3 fibroblast. Pathological and molecular analyses reveal unanticipated ligand-dependent phenotypes of the tumors including alterations in the expression of Notch receptors and effectors, supporting the hypothesis that unique functional roles exist for these ligands.

Materials and Methods

Cell Lines

The constructs and stable cell transfectants used in this study have been previously generated and characterized.[16,32,33] Pooled stable transfectants individually expressing hJag1,[32] hDl1,[16] sJag1,[35] sDl1,[16] or empty vector were used for these studies.

In Vivo *Tumor Allografts in Immunocompromised Mice*

All protocols involving mice were evaluated and approved by our Institutional Animal Care and Use Committee, and performed under veterinary supervision. The *in vivo* model for subcutaneous tumor development in nude mice was performed as described[36] with the exception that the cell suspension was supplemented with a basement membrane extract. Briefly, NIH3T3 stable lines were grown to confluence in Dulbecco's Modified Eagle's Medium containing 10% bovine calf serum (Hyclone Laboratories, Logan, UT), 1× antibiotic/antimycotic (Hyclone Laboratories, Logan, UT), and 100 μg/ml Genticin (Invitrogen, Carlsbad, CA). For injection, the transfectants were washed twice with PBS, trypsinized and centrifuged at 450 × *g* for 3 minutes to pellet the cells. After removal of the supernatant, the cellular pellets were resuspended in PBS mixed with 100 μl of Matrigel (BD Bioscience, San Jose, CA). Male athymic nude mice (*nu/nu*) from Taconic Farms, Inc. (Germantown, NY) 6 to 8 weeks of age were injected subcutaneously in the right flank with 2×10^6 transfected cells in a total volume of 200 μl. Tumor growth was monitored by palpation, and the onset noted when tumors were palpable. Tumor size was measured with calipers, and tumor volume calculated assuming the shape as ellipsoid. Representative data were obtained from five mice/experimental group, and the entire experiment was repeated in three independent trials. Before collection, mice were injected subcutaneously with 200 μl of 25 mg/ml bromodeoxyuridine (BrdU) solution at 15 hours and 1 hour before collection. The mice were euthanized and the tumors and overlying skin collected 3 to 5 weeks after injection, depending on growth. After the tumors were individually weighed, approximately half of the mass was snap frozen for mRNA and protein analysis with the remaining half cryofrozen in OCT embedding media (Electron Microscopy Sciences, Hatfield, PA) or fixed in 4% paraformaldehyde and embedded in paraffin for histological studies.

Histology and Immunohistochemistry

Paraffin-embedded tissue samples were cut into 5 micron sections using a microtome for pathological analysis as well as BrdU, platelet endothelial cell adhesion molecule-1 (PECAM), and terminal UTP nicked-end labeling (TUNEL) immunostaining. For pathological analysis, sections were stained with H& E or Masson's trichrome for visualization of connective tissue. At least five slides per tumor sample were analyzed for each stain by a board-licensed veterinary pathologist in a blinded manner.

For BrdU immunostaining, deparaffinized serial sections were treated with 0.3% H_2O_2 in methanol at room temperature for 20 minutes, followed by treatment with 20 mg/ml proteinase K in 50 mmol/L Tris/5 mmol/L EDTA for 7 minutes at room temperature. Immediately following proteinase K treatment, cells were washed in 0.4% glycine/PBS, and then incubated in 1.5N HCl for 15 minutes at 37°C. Cells were then washed in 0.1M borax buffer, and immunostained with a 1:100 dilution of anti-BrdU (MP Biomedicals, Solon, OH), followed by incubation with a biotinylated anti-mouse antibody. The antigen was detected using the ABC Elite reagent (Vector Laboratories, Burlingame, CA) using diaminobenzidine as the color substrate. For quantification of BrdU-positive cells, 10 random fields (magnification ×40) were captured for each sample, and the percentage BrdU labeled cells determined by counts of labeled/total cells.

The TUNEL method was used to determine number of apoptotic cells within each section. Deparaffinized serial sections of the tumors were labeled with biotin dUTP using terminal deoxynucleotidyl transferase (TdT) to detect DNA fragmentation. Following 3% H_2O_2 treatment and proteinase K antigen retrieval, tumor sections were incubated for 1 hour at 37°C in TdT reaction solution (TdT 0.25U/ml, biotin-dUTP 0.4nmol/ml in TdT Buffer [30 mmol/L Tris-base pH = 7.2, 140 mmol/L sodium cacodylate, 1 mmol/L cobalt chlo-

ride]). TdT activity was then quenched with incubation in TdT reaction termination buffer (300 mmol/L NaCl, 30 mmol/L sodium citrate). Antigen was detected using the ABC Elite Reagent (Vector Laboratories, Burlingame, CA) and diaminobenzidene as the color substrate. Quantification of TUNEL-positive cells was performed as described for BrdU immunostaining.

Immunostaining for endothelial cells on deparaffinized serial sections was performed with anti-PECAM antibodies (BD Biosciences, San Jose, CA) using a biotinyltyramide amplification reagent (Perkin Elmer, Waltham, MA) and diaminobenzidine as the color substrate. Non-counterstained PECAM sections (five tumors per condition) were quantified for vessel area. Nine to ten pictures of comparable regions of each tumor were taken and quantified in a blinded fashion. Using Photoshop 7.0, the vessels were outlined in a transparent layer and filled in with black. The outlined vessel image was opened in Scion Image, converted to binary, threshold set to constant, and area of black pixels measured. Shown is average percentage of vessel area per tumor area, and results were analyzed by Student's *t*-test to determine statistical significance compared to the control group.

Oil Red O was performed on 25 micron serial cryosections of the tumors as described.[37] Briefly, sections were air dried, fixed in 10% neutral formalin for 5 minutes and rinsed in distilled water before placing the slides in an Oil Red O solution (3:2 dilution Oil Red O stock to ddH_2O; Oil Red O stock solution is 3 mg/ml in isopropanol) for 8 minutes at 60°C. Slides were then rinsed in distilled water and counterstained with hematoxylin.

Quantitative and Qualitative RT-PCR

Total RNA was collected using TRI Reagent (Sigma, St. Louis, MO) following the manufacturer's protocol. RNA was reverse transcribed using oligodT in the presence of avian myeloblastosis virus reverse transcriptase to make cDNA. Successful cDNA production was verified by PCR (PCR Master Mix, Eppendorf North America, Westbury, NY) using primers against *β-actin* (forward, 5′-GGAGGAAGAGGATGCGGCA-3′, reverse, 5′-GAAGCTGTGCTATGTTGCTCTA-3′). Qualitative PCR on vascular endothelial growth factor A (*VEGF*)*A* (forward, 5′-CAGAAGGAGAGCAGAAGTCC-3′, reverse, 5′-CTCCAGGGCTTCATCGTTA-3′); *VEGFB* (forward, 5′-CCCAGTTTGATGGCCCCA-3′, reverse, 5′-TGCCCATGAGTTCCATGC-3′); *VEGFC* (forward, 5′-GTAAAAACAAACTTTTCCCTAATTC-3′, reverse, 5′-TTTAAGGAAGCACTTCTGTGTGT-3′); and *VEGFD* (forward, 5′-GCAAGACGAGACTCCACTGC-3′, reverse, 5′-GGTGCTGAATGAGATCTCCC-3′), as well as the receptors *VEGFR1* (forward, 5′-TCAGCAGCTCAAGTGTCACC-3′, reverse, 5′-GCTGCTTGGAGATCTCACTG-3′); *VEGFR2* (forward, 5′-ATGACATCTTGATTGTGGCAT-3′, reverse, 5′-TTCCAGATGCTGGGCAAGTC-3′); and *VEGFR3* (forward, 5′-GCAGGAGGAGGAAGAGGAGC-3′, reverse, 5′-TGCATGCTGGGTGGACTATCA-3′) was performed using primer sets as indicated. PCR products were visualized by gel electrophoresis and staining with ethidium bromide.

Quantitative real-time PCR (qRT-PCR) was performed on tumor cDNA using the Taqman Fast System and reagents (Applied Biosystems, Foster City, CA) per manufacturer's instructions. Applied Biosystems murine-specific Gene Expression Assay sets used for these studies were as follows: *β-actin* (#Mm00607939_s1); *delta1* (#Mm00432841_m1); *fabp4* (#Mm00445880_m1); *fas* (#Mm0066319_m1); *hes1* (#Mm01342805_m1); *hes3* (#Mm00468603_m1); *hes5* (#Mm00468865_g1); *hey1* (#Mm0046865_m1); *hey2* (#Mm00469280_m1); *hprt* (#Mm01545399_m1); *jagged1* (#Mm00496901_m1); *lipoprotein lipase* (#Mm00434764_m1); *notch1* (#Mm00435245_m1); *notch2* (#Mm00803077_m1); *notch3* (#Mm00435270); *notch4* (#Mm00440525_m1); and *pparγ* (#Mm00440945_m1). Quantitative analysis of the real-time data was performed using the comparative Ct method (Applied Biosystems SDS Software package) with either *β-actin* or *hprt* used as the endogenous control. At least two separate assays from different cDNA stocks, each with a minimum of three replicates were performed for every comparative study (relative expression). Significance was determined using either analysis of variance and/or Student's *t*-test.

Angiogenesis Blot Assay

Detection of blood angiogenic factors in mice bearing NIH3T3 allografts was performed using the TransSignal Angiogenesis Antibody Array (Panomics, Fremont, CA) following the manufacturer's instructions using cell free plasma. Blood was collected from mice by eye bleed into EDTA-coated microcontainers (BD Bioscience, Franklin lakes, NY). Plasma was separated from the blood cells by centrifugation at 7000 × *g* for 10 minutes. Samples were stored at −20°C until use.

Immunoblot and Enzyme-Linked Immunosorbent Assay Analysis

Total cell lysate for immunoblot and enzyme-linked immunosorbent assay (ELISA) analysis was prepared using the Pressure Cycling Technology with the Barocycler NEP-3229 instrument (Pressure BioSciences, Inc., South Easton, MA.) as described.[38] The cell lysis buffer used in the extraction consisted of 150 mmol/L NaCl, 50 mmol/L Tris pH = 8, 1% Triton X-100, and proteinase inhibitors. Samples were analyzed by SDS-polyacrylamide gel electrophoresis, transferred to nitrocellulose membrane, and immunoblotted with reagents as indicated. Antibodies specific for the intracellular domain of Notch receptors were Notch1 (C-20), Notch2 (M-20), Notch4 (H-225) (Santa Cruz Biotechnologies, Santa Cruz, CA), and Notch3 (EP2433Y) (Epitomics, Burlingame, CA). Immunoblots were visualized using chemiluminescence (Amersham Biosciences, Piscataway, NY). The VEGFA ELISA analysis was performed on the cell lysates using the Mouse VEGF Duo set (R&D Systems, Minneapolis, MN) as per manufacturer's instructions. Protein concentrations of each lysate were determined using a modified bicinchoninic acid method (Pierce, Rockford, IL) as per manufacturer's instructions.

Magnetic Resonance Imaging and ^1H Spectroscopy

Axial and coronal images through the tumor area were acquired from isoflurane (1%, 0.4 l/min) anesthetized

mice in a 7.0T Bruker PharmaScan magnet. A rapid acquisition method with enhanced relaxation was used (TR 2500 ms, TE 10.64 ms, FOV 3.5 cm, matrix size 256 × 256, slice thickness 1 mm, total scan time, 5 minutes 30 seconds). The tumor dimensions were measured at the largest width, length, and height. For localized spectroscopy Point Resolved Spectroscopy (TR 2000 ms, TE 21.4 ms) was used. A voxel of 1 mm^3 was placed into the center of the tumor. Placement of the voxel had no influence on the spectrum. One spectrum is the sum of 800 fields with a total scan time of 26 minutes 40 seconds.

Results

Ligand Expression Alters the Complement of Notch Receptors and Downstream Effectors in Tumors Derived from NIH3T3 Cells

We previously reported that suppression of Notch signaling by extracellular and soluble forms of the Notch ligands Jagged1 and Delta1 induced transformation of NIH3T3 cells *in vitro*.[16,32,33] *In vitro*, the soluble forms of these ligands were shown to suppress canonical Notch signaling using a well-established luciferase reporter assay that measures Notch/CBF1 transcriptional activity.[39] In addition, NIH3T3 cells exposed to the conditioned media of sJag1 and sDl1 cells also incur a reduction in CBF1-mediated luciferase assay (data not shown), further indicating that the soluble forms of these ligands do interfere with Notch/CBF1 activity in this cell model. To determine whether these ligands also induced transformation of NIH3T3 fibroblasts *in vivo*, we studied the characteristics of tumors generated from NIH3T3 transfectants stably expressing either soluble (sJag1, sDl1) or full-length forms (Jag1, Dl1) of Jagged1 and Delta1, respectively, after injection into immunocompromised (*nu/nu*) mice. In addition to the cellular suspension, we also added basement membrane extract to the injection cocktail as it has been reported to support the growth of solid tumors in this model.[40] As described throughout this report, we found that tumor growth occurred from all injected cell lines except for those expressing full-length Jagged1 over the course of the study. In addition, considerable differences in tumor phenotype from each cell line were observed. Since the only initial variable in these studies was the nature of the Notch ligand constitutively expressed by the NIH3T3 cell, we assayed the tumors for Notch receptor activity to determine the effect that ligand identity had on this system. First, we analyzed relative expression of steady-state Notch receptor mRNA among the tumor types to determine whether ligand expression was associated with changes in Notch receptor populations within the tissue. Using qRT-PCR, we found the full complement of Notch receptors (Notch1, Notch2, Notch3, and Notch4) expressed in all tumors with sJag1 tumors expressing the highest mRNA levels of all Notch receptors among the tumor types (Figure 1A). Notch receptor mRNAs in Dl1 allographs were significantly lower (Notch1, Notch2) or unchanged (Notch4) from the NIH3T3 control samples (Figure 1A). Notch1 and Notch3 were also elevated in the sDl1 samples compared to control (Figure 1A). Together, these data suggest that soluble forms of the ligands may promote the transcription or extend the half-life of mRNAs for the receptors, perhaps as part of a feedback loop designed to balance a normal Notch response.

The ability of the soluble and full-length ligands to promote or repress Notch cleavage within the mature tumors was examined by immunoblot analysis using antibodies that recognize the intracellular domain of each

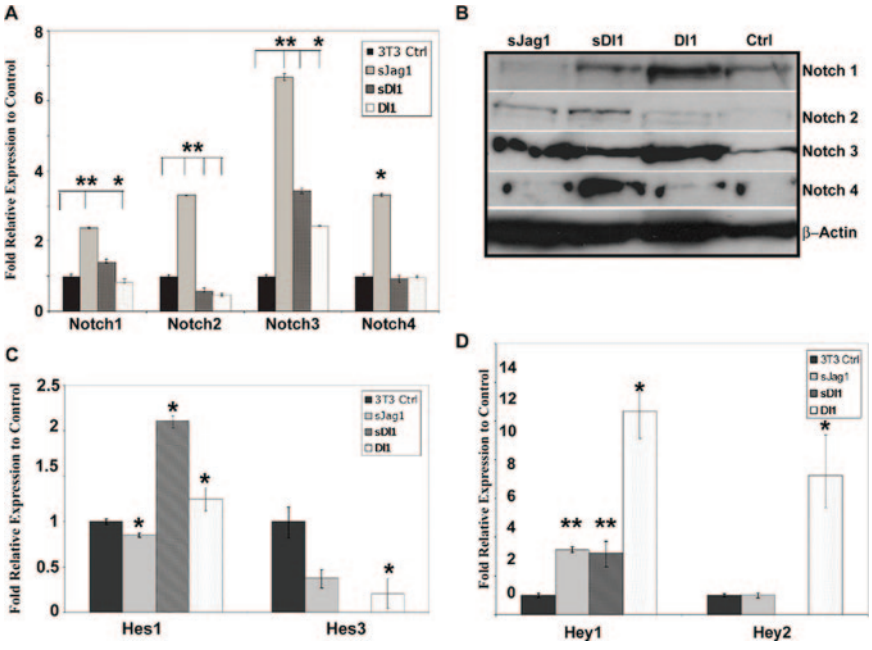

Figure 1. Ligand expression alters Notch receptor activity and expression of downstream effectors in tumors derived from NIH3T3 cells. **A:** Quantitative RT-PCR (Taqman) was performed to determine expression levels of transcripts for each Notch receptor as indicated. cDNA was generated from total RNA isolated from at least three individual tumors from each group. Quantitative PCR was performed for each sample in triplicate and quantitative analysis of the real-time data was performed using the comparative Ct method (ABI SDS Software package) with β-actin used as the endogenous control. Data are presented as fold expression in comparison to NIH3T3 control (value of "1") for each assay. Error bars represent the 95% maximum and minimum confidence limits. One-way analysis of variance was used to determine significant differences between samples in comparison to control for each expression assay. Significant differences between the target sample and control are indicated with * representing $^*P < 0.5$ and $^{**}P < 0.001$. **B:** Immunoblot analysis for the presence of proteolytic fragments representing the cleaved intracellular domain for each Notch receptor was performed as described in Materials and Methods. Immunoblot analysis for β-actin (bottom panel) was used as a loading control. **C and D:** Quantitative RT-PCR (Taqman) was performed as described in (**A**) to determine expression levels of transcripts for the Notch effectors (Hes1, Hes3, Hey1, Hey2) for each tumor type as indicated.

receptor. Semiquantitative analysis of positive bands with molecular weights corresponding to the cleaved intracellular domain of the receptor indicated that tumors derived from Dl1 transfectants displayed the strongest signal for both the Notch1 and Notch3 receptors, as expected (Figure 1B). In contrast, samples extracted from sJag1-derived tumors displayed a general reduction of all Notch receptor cleavage products with the exception of Notch 3. Interestingly, lysates from sDl1 allographs also contained measurable quantities of cleaved Notch1 and Notch2 that were relatively higher than the 3T3 control (but not Dl1 transfectants) as well as a Notch4 band that was more intense than any other sample. To further explore the nature of Notch signaling status within the tumors, we used qRT-PCR to determine the relative expression of the Hes (Hes1, Hes3, Hes5) and Hey/HRT (Hey1, Hey2) family of Notch effectors (Figures 1C and 1D, respectively). Hes1 mRNA abundance was 2 to 10-fold higher than Hes3, depending on tumor type, and generally greater than 20-fold higher or more than either Hey1 (HRT1) or Hey2 (HRT2). Hes5 mRNA was not detectable in any of the tumors (data not shown). Both sDl1 and Dl1 tumors expressed significantly higher Hes1 mRNA than control with sJag levels modestly, but significantly, depressed (Figure 1C). Interestingly, the relative abundance of mRNA for both Hey1 and Hey2 in the Dl1 tumors was greater than eightfold higher than control, suggesting that Dl1 may preferentially stimulate expression of these effectors in this model. sDl1 increased Hey1 similarly to sJag1 and had the unique characteristic of producing tumors completely devoid of detectable mRNA levels for either Hes3 or Hey2. Together, these data indicate that the signaling status of the Notch receptors and their effectors differed among tumor types, most likely due to the effects that the exogenous ligands had on Notch receptor expression and/or activation in the parental and/or recruited (endogenous) tumor cells since this was the only starting variable among the experimental conditions. It is of importance to note that while soluble forms do suppress Notch signaling *in vitro*, these data must also be considered in light of the fact that the cellular composition of the tumors do not consist entirely of our transfected cells, but instead are populated by other endogenous cell types including endothelial cells that will also contribute to the pool of total mRNA and protein found within the tissues. In addition, it has been reported that whether or not soluble forms of the ligands are agonists or antagonists is dependent on the ability of the ligand to dimerize and it is possible that sDl1 and to a lesser extent, sJag1 may be able to do so via interactions with the extracellular matrix.

Expression of Soluble Notch Ligands Increases the Tumorigenicity of NIH3T3 Cells

Palpable tumors developed from cells expressing the soluble ligands (sJag1 and sDl1) at a strikingly earlier time period than those generated from cell lines expressing empty vector or full-length Dl1 (Figure 2A). Tumor onset occurred on average 8 and 12 days after injection of sJag1 and sDl1 populations, respectively, compared

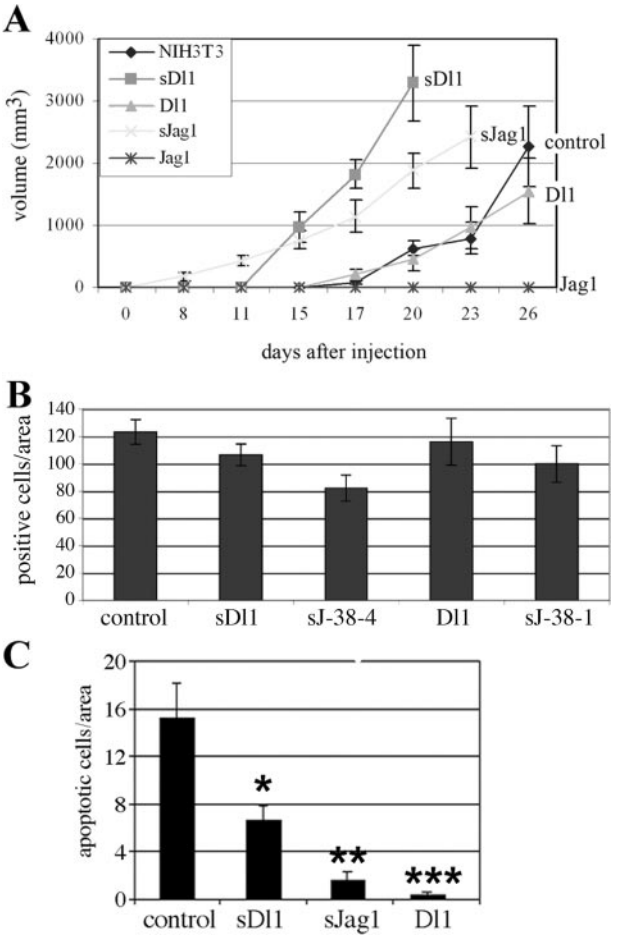

Figure 2. Suppression of Notch signaling in NIH3T3 cells enhances *in vivo* tumorigenicity. **A:** NIH3T3 cells stably expressing either full-length Jagged1 (Jag1), Delta1 (Dl1), or soluble forms of each (sJag1 and sDl1, respectively) were grown subcutaneously in athymic nude mice. Tumor volume was measured using a caliper over the course of 26 days after injection. **B:** Cell proliferation was measured in the tumors by counting the number of cells/field in 5 μmol/L serial sections that stained positive with an anti-BrdU antibody. For quantification of BrdU-positive cells, 10 random fields (magnification = original $\times$40) were captured for each sample and data are presented as number of BrdU-labeled cells/area. Shown are means $\pm$ SEM. **C:** The TUNEL method was used to determine number of apoptotic cells/field within 5 μmol/L serial sections of the tumors. Quantification of TUNEL-positive cells was performed as described for BrdU and is reported as number of TUNEL-positive cells/area. Shown are means $\pm$ SEM. Significance was determined by one-way analysis of variance for each tumor type in comparison to NIH3T3 control. The number of TUNEL-positive cells were found to be significantly different in all cell lines. Asterisks represent P values *$<$0.05; **$<$0.01; ***$<$0.001.

to $\sim$17 days after injection for the control and Dl1 lines. The Dl1 population behaved similarly to the empty vector control, with both groups forming tumors greater than 1500 mm^3, but only $>$35 days after injection. In contrast, the Jag1 transfectants failed to form tumors, even 8 weeks postinjection (data not shown), supporting a role for this ligand as a potent tumor inhibitor in this model. Jagged1 transfectants also failed to form colonies in soft agar (data not shown), further substantiating its role as a tumor suppressor in the NIH3T3 fibroblast. In contrast, NIH3T3 cells stably transfected with a dominant negative form of CBF-1 formed highly angiogenic tumors 12 to 18 days after injection, supporting the hypothesis that suppression of canonical Notch signaling promotes the tu-

morigenicity of these cells (I. Prudovsky, personal communication). Since injection of Matrigel alone also did not lead to tumor growth (data not shown), it is likely that tumor development was due to the presence of the exogenous transfectants and not primarily by recruitment of endogenous cells due to growth factors present in the basement membrane extract.

To assess if the growth dynamics of each allograft reflected an increase in cellular proliferation and/or survival, we performed both BrdU incorporation and TUNEL assays, respectively. Surprisingly, staining of the tumors for BrdU incorporation indicated that no significant differences ($P > 0.05$) were found in the percentage of mitotic cells within each tumor (Figure 2B). These results were also confirmed by histological examination of the tumors, which revealed only 4 to 11 mitoses per ×400 field, with sJag1-derived outgrowths having slightly more mitoses than the other lines. These results were also consistent with cell cycle analysis of cultured transfectants in which we found that more than 80% of the cells were in G1 phase in all of the cell lines tested from 0 to 8 hours. The vector control, Jag1, Dl1, sDl1, and sJag1 cells showed a similar cell progression up to 28 hours through G1, G2 and S (data not shown). Interestingly, unlike the other lines that did not maintain synchronicity after 28 hours, the cell cycle progression of the Jag1 population remained synchronized throughout the experiment with almost all cells being in the same phase at any given point (data not shown).

Since tumor growth reflects the net difference between cell proliferation and death, we also assessed apoptosis using a standard TUNEL assay. Evidence of DNA fragmentation was greatest in the control tumor, followed by sDl1, sJag1, and surprisingly, the Dl1 tumors (Figure 2C). These results suggest that the fast development of the tumors derived from the soluble ligands may be due, in part, to a decreased response to apoptotic signals. Although the proliferation and apoptotic indices did not strictly correlate with final tumor size, a consideration in the interpretation of the BrdU and TUNEL labeling is that these were end-point analyses performed at the time of maximal tumor size and therefore did not reflect growth or apoptosis occurring in the log phase of tumor development.

Ligand Expression Controls Tumor Phenotype

Although ectopic expression of all ligand constructs with the exception of full-length Jag1 increased the tumorigenicity of the NIH3T3 cell, expression of sDl1 resulted in tumors that formed earlier and grew faster than those produced by the other cell lines (Figure 2A). To further delineate phenotypic differences among the tumors, we performed a pathological examination of H&E and Masson's trichrome-stained serial sections of each of the tumors generated in the study. First, we observed that all tumors were highly compact and were primarily composed of bundles of spindloid mesenchymal cells (Figure 3). The spindloid cells of all tumors were found, in general, to have finely stippled or hyperchromatic nuclei with 0 to 3 small nucleoli. However, the chromatin in cells within the sJag1-derived tumors was sometimes found to be coarser than that observed in control, sDl1-, and Dl1-derived growths. Anisocytosis and anisokaryosis were moderate in control, sDl1, and sJag1 tumors and mild to moderate in Dl1 tumors, indicating that all displayed some degree of pleiomorphism.

Despite these similarities, pathological examination revealed marked structural differences among the tumors derived from the stable NIH 3T3 transfectants (Figure 3). The tumors differed significantly in several aspects, most notably in degree of necrosis, vascularization (Figure 3 and 4A), and invasion into adjacent tissue. Tissue necrosis was most prevalent in the NIH3T3 control-derived tumors, which were characterized by mild to marked focal necrosis with mild hemorrhage from the surrounding vessels in 75% of all sections (Figures 3, A–C, and 4A). Surprisingly, necrotic foci were smaller and fewest in number in the Dl1 derived outgrowths, with only 30% of the sections displaying the presence of minimal to mild focal or multifocal necrosis (Figure 3, J–L). The percentage of sections showing significant necrosis was 62% in sDl1, 55% in sJag1, and 30% in the Dl1 tumors. These results suggest that while expression of the soluble ligands increased the initial proliferative potential or survival of the NIH3T3 cells, the Dl1-expressing cells developed into tumors that were less susceptible to necrosis or apoptosis-inducing factors such as limited nutrient and oxygen availability.

Since angiogenesis is critical for preventing necrosis and sustaining tumor development, we next examined the vascular structure of the outgrowths to determine whether ligand expression impacted the vascularization of the tumors. While angiogenesis occurred in all tumors examined, the quality and quantity of neovessel formation within tumor types differed extensively (Figures 3 and 4). For example, in NIH3T3 control-derived tumors, microvessels were the least mature and found to be predominately open-ended, discontinuous and associated with the presence of extravascular blood, especially near the periphery of the tumor (Figures 3A, and 4A). Progressive increased arborization and sprouting of the vessels were observed toward the center of the tumors and on the periphery of necrotic areas. Some vessels within these tumors were also often found to be congested with fibrin thrombi (Figure 3B), especially in those adjacent to the necrotic foci of the tumor. Of the stable transfectants, the vessel phenotype of sDl1 tumors were most like the NIH3T3, although the vasculature within these tumors did begin to arborize more peripherally, displayed more branches and were associated with less extravascular blood than control tumors (Figures 3D, E, F and 4A). Vessels near the necrotic foci were also congested, but the presence of fibrin thrombi was more infrequent in these tumors than in the controls. The sJag1 tumors displayed a vascular network that was more extensive than those observed in either the control or sDl1 tumors (Figures 3H and 4A). The vessels of these tumors were, on average, more dilated than those found in all of the other allographs and accordingly, were the least congested with fibrin thrombi. Interestingly, mild focal interstitial edema was observed in areas adjacent to some of the larger vessels, indicating that these vessels were

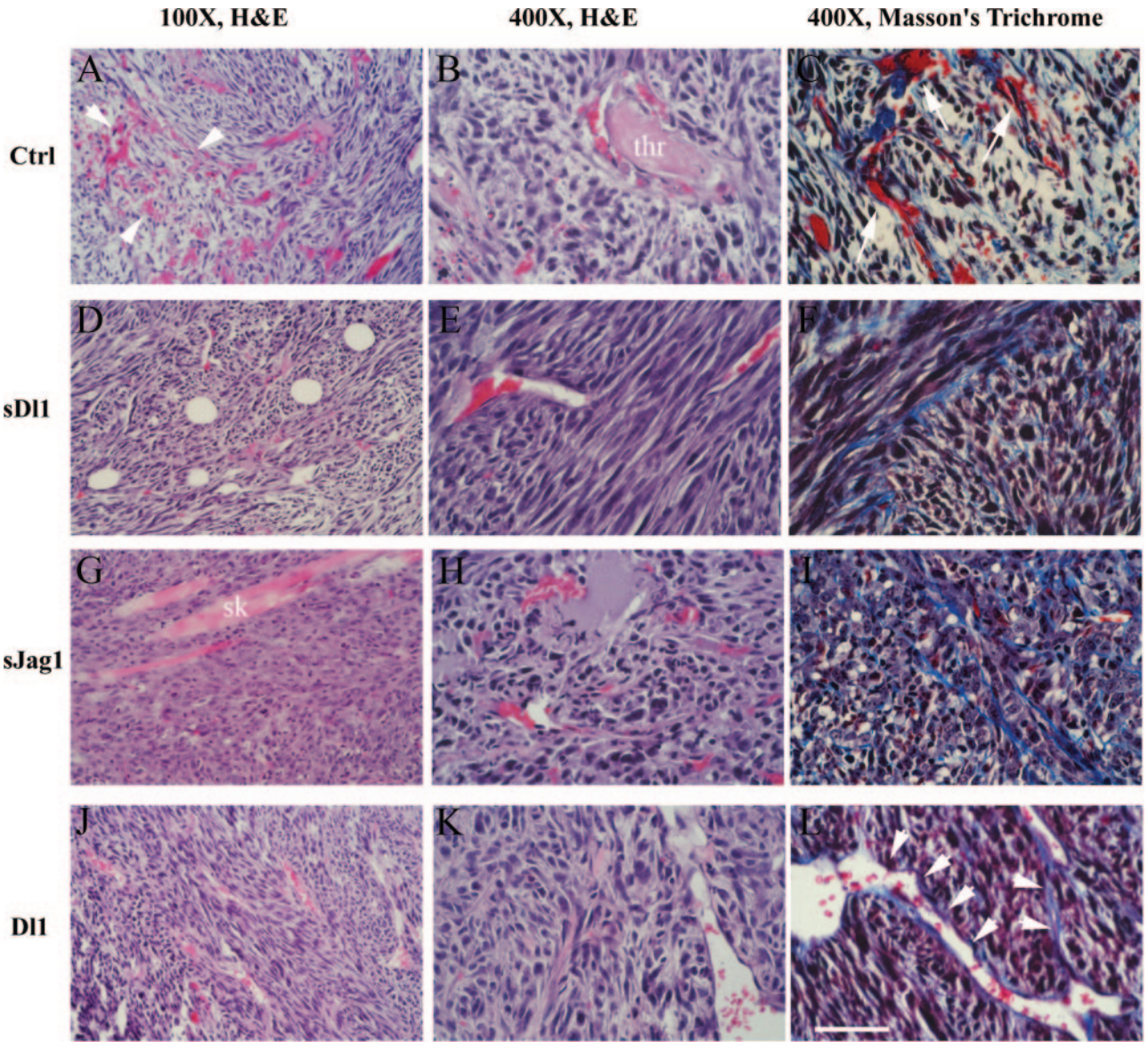

Figure 3. Notch ligand expression alters tumor morphology. Tumor specimens were fixed, embedded in paraffin, sectioned, and stained with H&E (left two columns) or Masson's trichrome stain (right column). Samples represent control (**A–C**), sDl1 (**D–F**), sJag1 (**G–I**), and Dl1 tumors (**J–L**). Representative areas are shown and described within the text. Scale bar = 100 μm for panels (**A**), (**D**), (**G**), (**J**), and 50 μm for all others. White **arrows** indicate vessels; thr = fibrin thrombi; sk = skeletal muscle.

leaky. Lastly, the Dl1-derived outgrowths contained the most mature vascular network of all tumor lines, with microvessel arborization consisting of an interconnected network of small to medium sized vessels found throughout the tissue (Figures 3, J–L and 4A). Observations of small vessels sprouting from medium sized vessels could be seen in several sections (Figure 3, J and K). In summary, we found substantial qualitative differences in the vascular network of tumors formed from each of the stable transfectants. These observations support unique functional roles for Notch ligands in the regulation of tumor angiogenesis.

Last, we noted variation in other tumor characteristics including collagen deposition. Microscopic analysis of Masson-trichrome-stained sections (Figure 3, C, F, I, L) revealed that collagen deposition was greatest in sDl1 followed by the controls. Both sJag1 and Dl1 had the least amount of collagen between mesenchymal cells, with only scant to small levels of staining observed within the sections. In addition, we also discovered some unusual characteristics associated with expression of the ligands, such as the presence of intracytoplasmic droplets of eosinophilic proteinaceous material in several sections of sDl1-derived tumors, only (data not shown). Tumors also differed substantially in their ability to infiltrate adjacent healthy tissue at the site of the allograph. Both sDl1 and sJag1 were invasive with the tumors engulfing areas of the adjacent skeletal muscle (Figure 3G) and adipose tissue, consistent with their size and growth rate.

Tumor Neovascularization Is Correlated to the Production of VEGFA and Other Angiogenic Factors

Angiogenesis is an integral part of tumorigenesis, and the role of Notch signaling in remodeling and maintaining the

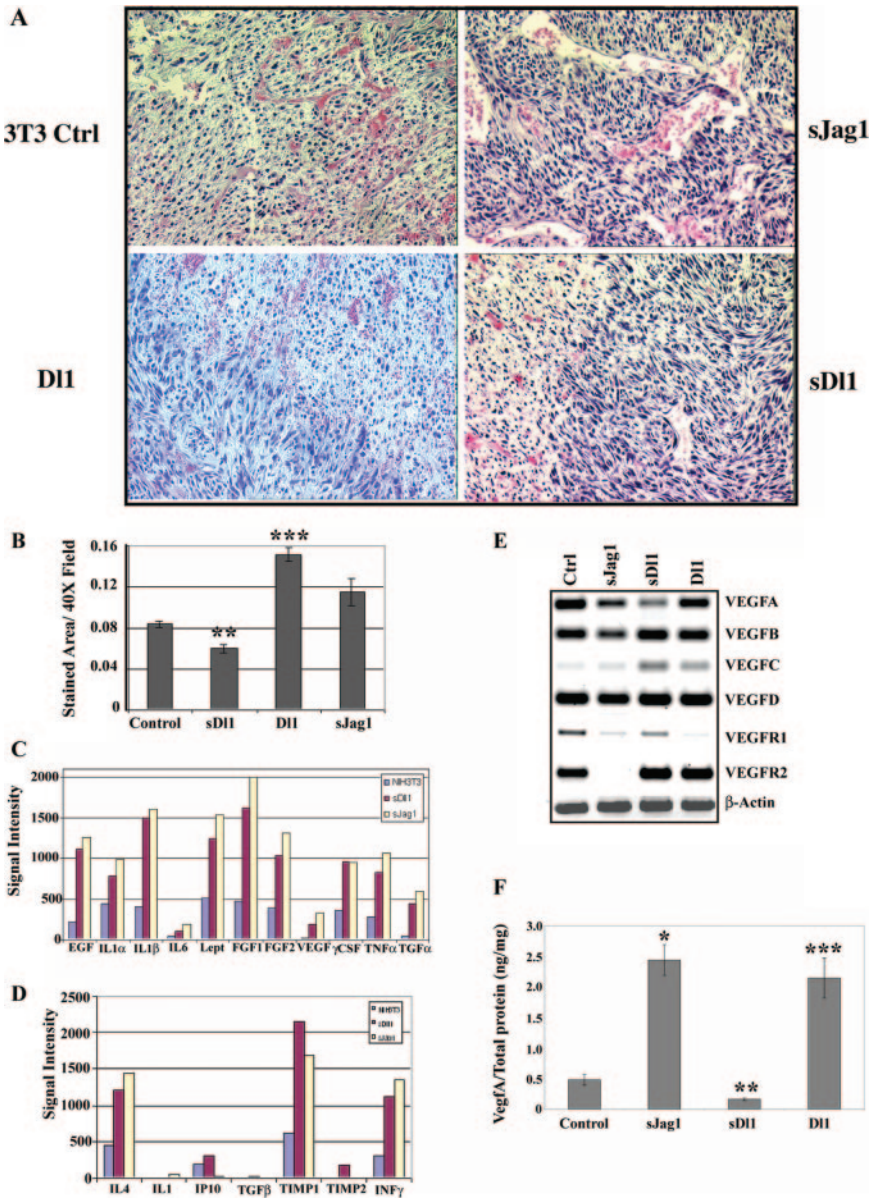

Figure 4. Notch ligand expression regulates tumor angiogenesis. **A:** Fixed and Masson's trichrome-stained tumor sections (magnification ×200) were analyzed for the presence of vasculature within the specimens. Vessels can be seen as pink steaks (smaller vessels) or in more dilated vessels, as clear areas containing red blood cells. **B:** 5 μm, paraffin-embedded tumor sections were immunostained with anti-PECAM to visualize and quantify vessel structure. Ten random fields (magnification ×40) were captured for each sample and data are presented as number of stained area per ×40 field. Shown are means ± SEM. Significance was determined by one-way analysis of variance for each tumor type in comparison to NIH3T3 control. The number of PECAM-positive cells was found significantly different from control in Dl1 and sDl1 tumors with P values of 0.0007 and 0.002, respectively. **C–D**) Plasma collected from tumor-bearing animals was processed for detection of positive regulators of angiogenesis (**C**) and angiogenic inhibitors (**D**) using an antibody array (Panomics) as described in Materials and Methods. Chemiluminescent signals from each array were captured by autoradiography and quantified by densitometry. Signals are reported as relative signal intensity. **E:** Total RNA was collected from tumor tissue to detect transcript levels of VEGF and VEGFR family members by qualitative RT-PCR. RT-PCR with actin primers was used as a control for cDNA synthesis. **F:** Expression of VEFGA in protein lysates isolated from tumors was quantified by ELISA per manufacturer's instructions. VEGFA is reported as the average of four individually processed tumor lysates for each type and is normalized to total protein in the sample as determined by bicinchoninic acid assay. Shown are means ± SEM. Significance was determined by one-way analysis of variance for each tumor type in comparison to control. VEGFA expression was found to be significantly different from control in all tumor types with P values of 0.001(sJag1), 0.009 (sDl1), and 0.01 (Dl1).

vasculature is well documented.[41,42] Since the initial pathological examination of tumor sections found marked differences in the extent, size and arborization of the vascular network (Figures 3 and 4A), we next quantified vessel density to determine how the expression of the Notch ligand constructs affected the global host response of angiogenesis (Figure 4B). Quantification of vessel density/tumor area using PECAM as a marker of blood vessel endothelial cells showed that in agreement with the observations made during pathological examination, vessel density was greatest in the Dl1-derived tumors (Figure 4B). Although pathological examination indicated that sJag1 had the lowest prevalence of microvessels, the quantitative analysis of PECAM-positive areas indicated that these tumors had the second highest vessel density of all tumor types and was likely due to the dramatically larger average size of sJag1 tumor vessels. sDl1 had the least amount of PECAM-stained area/section. Since these differences in vascularization could be due to differences in angiogenic cytokine production, we tested blood plasma levels for the presence of those typically thought to be positive (Figure 3C) or negative (Figure 3D) regulators. Blood was collected from tumor-bearing mice, and plasma assayed for circulating cytokines using an angiogenesis antibody array (Panomics, Fremont, CA). Array analysis indicated that the levels of angiogenic cytokines in the blood from mice bearing tumors derived from transfectants expressing soluble ligands (sDl1 and sJag1) were generally higher in comparison to control animals. The cytokine profiles from sDl1 and sJag1 mice were similar with sJag1 transfectants having the highest levels of all but one (G-CSF) of the pro-angiogenic regulators including epidermal growth factor, interleukin-1β, leptin, and fibroblast growth factor 1 and 2 (detection level over 100% of the positive control, Figure 3B). Next, we examined blood plasma

levels for the presence of anti-angiogenic factors in an attempt to understand the discrepancies we observed in vessel density and production of angiogenic factors among the experimental groups (Figure 3D). Among the negative regulators of angiogenesis, tissue inhibitor of metalloproteinase-1, and interferon-γ were up-regulated more than 15- and 5-fold, respectively, in animals injected with either of the soluble-ligand expressing cell lines. These results suggest that tumor growth altered the composition of serum angiokines that may have impacted their individual growth, survival and angiogenic properties. While these factors may also have had an influence on the metastatic potential of the tumors, we saw no gross evidence of metastases within the animals and unfortunately were unable to analyze other tissues microscopically for their presence.

VEGF family members are considered the quintessential angiogenic regulators as activation of their receptors influences the whole spectrum of the angiogenic process including remodeling, branching and control of vascular permeability.[43,44] Therefore, we examined tumor lysates for expression of VEGFA and other family members to determine whether ligand expression altered the production of these factors. Qualitative RT-PCR indicated that the all tumors analyzed expressed mRNA for VEGFA, VEGFB, and VEGFD, with only the sDl1 tumors expressing VEGFC at appreciable levels (Figure 4E). Although blood plasma levels of VEGF were only found to be mildly elevated in animals injected with the sJag1 and sDl1 transfectants (Figure 4B), we wanted to determine the status of VEGF signaling in the tumors themselves and therefore we performed an ELISA for VEGFA using tumor extracts (Figure 4F). The results from this assay indicate that both sJag1 and Dl1 extracts contained ~10-fold higher levels of VEGFA/mg total protein than either control or sDl1. Lastly, qualitative RT-PCR revealed that sJag1 expressed either barely detectable or undetectable levels of VEGF-R1 and VEGF-R2, respectively, although both of these receptors were found in control and sDl1-derived tumors. In summary, we observed marked differences in both the morphological characteristics of the tumor vasculature and production of angiogenic regulators among tumors produced by cell lines whose only genetic differences were the identities of the exogenously expressed ligand.

Expression of Soluble Notch Ligands Increases the Lipid Content of the NIH3T3-Derived Tumors

Pathological examination of the H&E-stained sections indicated the surprising presence of lipid-filled cells throughout the sJag1 and sDl1 tumors. To confirm that these vacuoles did contain neutral lipid, we performed Oil Red O staining of cryogenically-preserved serial sections (Figure 5). While all tumors were found to contain lipid stores within the skin and subdermal regions, there were striking differences in lipid accumulation within the tumor mass, proper. The control tumors had little detectable lipid, whereas the entire sDl1 tumor was populated by adipocyte-like cells harboring large lipid droplets (Figure 5, A and B). Interestingly, the sJag1 tumors had several cells containing small lipid droplets throughout the tumor (Figure 5C); however, the number of cells harboring these droplets was significantly less compared to the sDl1 tumor. The Dl1 tumors were, for the most part, negative (Figure 5D), although there were one to two small regions of strong lipid accumulation within the tumors (Figure 5D, inset). These findings of increased lipid accumulation in the sDl1 tumor were validated by localized spectroscopy as a method of measuring fat content in the tumors *in vivo*. Tumor-bearing mice were subjected to magnetic resonance imaging with subsequent measurement of fat within the tumor (Figure 5E). Consistent with the Oil Red O staining, the sDl1 tumors had a significant proportion of fat within the tumors in contrast to that found in sJag1 sections (Figure 5E). These results indicate that while expression of both soluble ligands produced lipid-bearing tumors, the overall amount of lipid stored differed significantly, possibly due to the influence of specific Notch/ligand interactions on triglyceride metabolism.

To further examine the possible relationship between ligand expression and the presence of these lipid-containing cells within the tumors, we performed qRT-PCR for the known adipocyte markers PPARγ, FABP4, Lipoprotein Lipase, and FAS (Figure 5F). While no significant differences were found in levels of PPARγ and its transcriptional target FABP4 among the tumor types, significantly higher levels of mRNA for Lipoprotein lipase and FAS were detected in the soluble ligand-derived growths in comparison to control and Dl1-derived tumors. Surprisingly, the sJag1 tumors expressed the highest levels of transcripts for these two enzymes important for fatty acid metabolism, suggesting that the ability of the sDl1 cells to accommodate larger droplets of intracellular lipid may also be due to some other as-yet-identified factor.

Discussion

The primary focus of this study was to determine the tumorigenic potential and functional differences of full-length and soluble forms of the Notch ligands Delta1 and Jagged1. While a fibroblast system such as the one used here does not reflect a true tumor model, it is nonetheless a well-documented method used to assay the oncogenic potential of genes.[45,46] Using this model, we found marked differences in the tumorigenicity of the Notch ligands Jag1 and Dl1. Unlike all other cell lines tested including control cells, Jag1 transfectants did not form tumors, even in the presence of Matrigel, indicating its role as a potent inhibitor of tumor growth in this system. It should be noted that in a previous study we reported that NIH3T3 control cells did not form tumors, and this difference is likely explained by the fact that the prior experiments did not use Matrigel, as in the present work.[35] In stark contrast to non-tumorigenic Jag1 expressing cells, Dl1 transfectants produced large, well-vascularized tumors with growth rates similar to tumors from the control cell lines. To study the former, expression of the extracellular domains of either Jag1 or Dl1 were used as

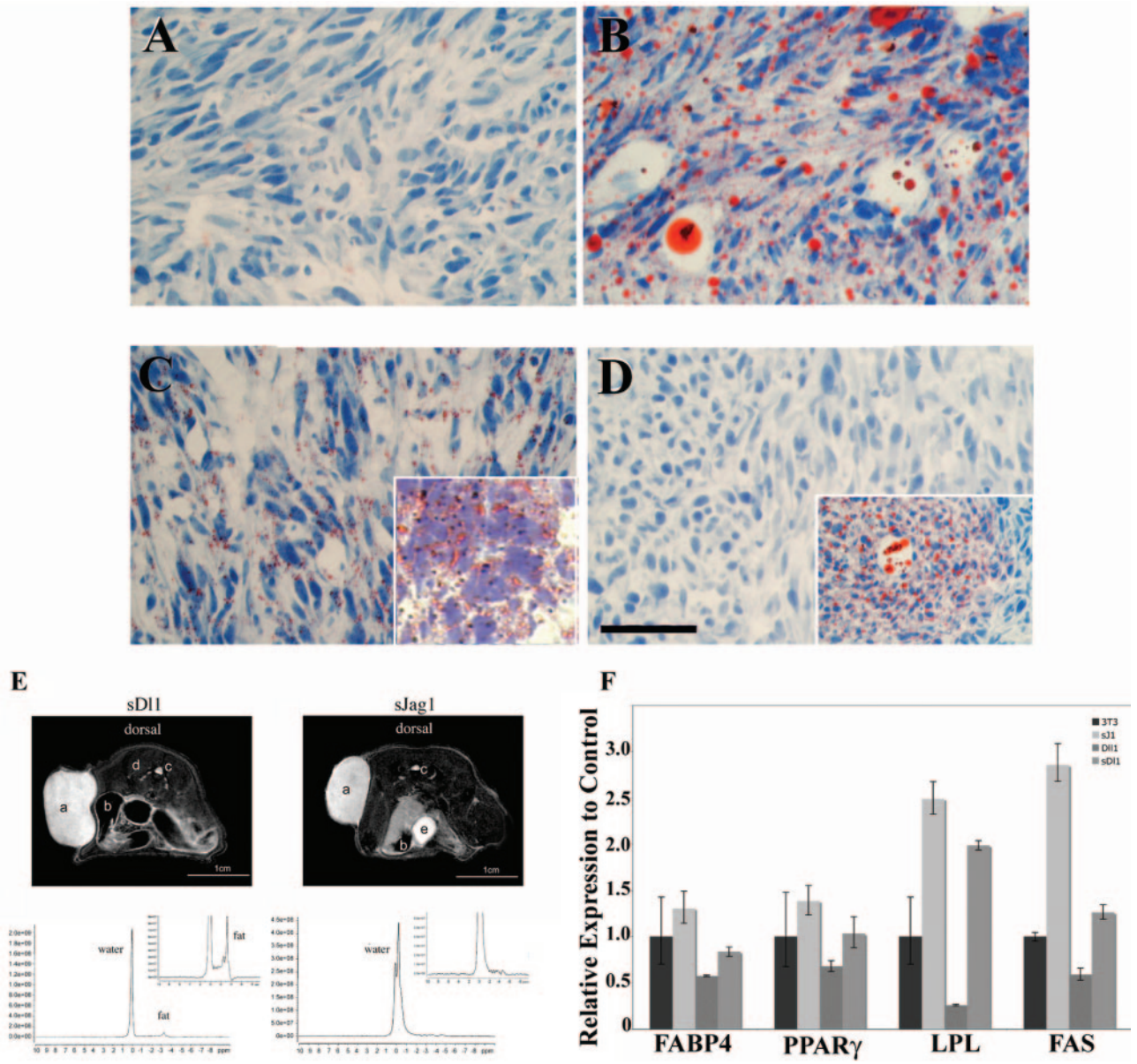

Figure 5. Expression of soluble forms of Notch ligands increases lipid accumulation in tumors. **A:** Tumors specimens were cryopreserved, sectioned, and stained with Oil Red O to detect neutral lipids. No internal lipid was detected in the control tumors (**A**), whereas lipid droplets were found throughout the sections of sDl1 tumors (**B**). sJag1 had low levels of spotty lipid accumulation marked by the formation of small droplets (**C** and **inset**) and Dl1 tumors (**D**), although predominantly negative throughout, had one to two small regions of lipid accumulation per tumor (**inset**). Scale bar = 50 μm. **E:** Magnetic resonance imaging and localized spectroscopy of tumors *in vivo* was performed to evaluate tumor growth and lipid content. Images are of representative of mice bearing a tumor derived from either sDl1 or sJag1 transfectants as indicated. Top panel represents axial images through the tumor area acquired from isoflurane-anesthetized mice in a 7.0T Bruker PharmaScan magnet. Tumors (a), intestines (b), spinal cord (c), muscle (d), and bladder (e) are indicated. The bottom panel represents localized spectroscopy with PRESS (TR 2000ms, TE 21.4ms) as acquired using a voxel of 1 mm^3 placed into the center of the tumor. Placement of the voxel had no influence on the spectrum. One spectrum is the sum of 800 fields with a total scan time of 26 minutes 40 seconds. Scans were done at 20 days after injection of cells. The water and fat peak are indicated. **F:** Quantitative RT-PCR was performed to determine expression levels of transcripts for genes important for lipid metabolism. cDNA was generated from total RNA isolated from at least three individual tumors from each group. Quantitative PCR was performed for each sample in triplicate and quantitative analysis of the real-time data was performed using the comparative Ct method (ABI SDS Software package) with β-actin as the endogenous control. Data are presented as fold expression in comparison to control for each assay. Error bars represent the 95% maximum and minimum confidence limits. One-way analysis of variance was used to determine significant differences between samples in comparison to control for each expression assay. Significant differences ($P < 0.001$) in Lipoprotein Lipase and FAS expression but not PPARγ and FABP4 were found for all samples in comparison to control.

suppressors of endogenous Notch signaling.[16,32] As predicted from *in vitro* studies where both sJag1 and sDl1 cause cell transformation,[16,33] tumor onset, growth rate, and final size of both soluble ligand-derived tumors exceeded those formed from control and full-length transfectants. However, tumor pathology was distinct, demonstrating that activation or suppression of Notch signaling through different ligands or their extracellular domains drives unique phenotypic outcomes *in vivo* (Figure 6).

The ability of the Notch signaling system to promote a tumorigenic versus a tumor suppressor activity is well appreciated,[34,47,48] although there is limited information regarding the functional contribution of the ligand specifically in cellular transformation. It is clear from our studies

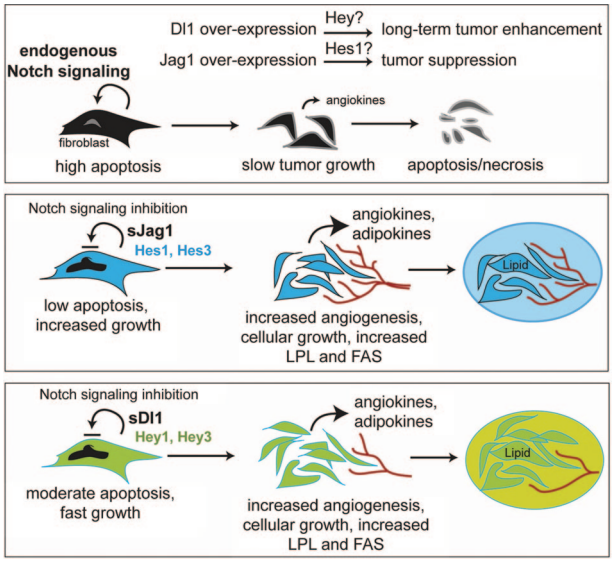

Figure 6. Ligand-induced modulation of tumor phenotype may be attributable to changes in Notch signaling cascades and expression of downstream effectors. In this model, endogenous Notch signaling in NIH3T3 control cells promotes apoptosis, slowing tumor growth. While angiogenesis does occur due to the modest production of angiokines, the extent and structure of the vascular network is limited, resulting in tumors with highly necrotic centers (**top panel**). Stimulation of Notch receptors by overexpression of full-length forms of the Jag1 and Dl1 ligands cause markedly different outcomes with Jag1 acting as a tumor repressor, possibly through stimulation of Hes1 and Dl1 producing slow-growing, well-vascularized tumors that may be supported by increases in Hey1 and Hey2 expression. In contrast, suppression of Hes and Hey effectors by soluble forms of Jag1 (**middle panel**) and Dl1 (**bottom panel**), respectively, confers either a resistance to apoptotic signals or possibly a change in proliferation that allow the cells to develop quickly into a relatively large mass capable of generating a vascular system that allows its growth to be sustained. Suppression of endogenous Notch signaling by the soluble ligands may further support growth by enhancing lipid metabolism of cells contained within the tumors.

that Jag1 and Dl1 are functionally distinct, a finding that is not unexpected given that the identity of the activating ligand has been demonstrated to alter Notch signaling events during development and in cellular differentiation.[15,16,49] For example, Jagged1 and Delta1 were shown to have unique functions during development of the sensory patches in the inner ear,[50] and distinct activities of Jag1 versus Dl1 have been identified in hematopoietic cells and their stromal compartment.[51,52] Distinct phenotypic pathways driven by Jagged1 and Delta1 have also been identified *in vitro* in leukemia cells,[53] however, have not been explored during *in vivo* tumorigenesis.

The diverging tumorigenic effect of expression of the individual ligand constructs may be attributed to their differential/preferential binding to the four Notch receptors and/or their ability to trigger down stream effectors. The tumor-promoting or -suppressing activity of the Notch signaling system has been reported to reflect the identity of the Notch receptors that are stimulated and cellular context.[54] For example, Notch1 activation causes arrest of cell cycle progression in chicken B-cell line DT40[55] as well as in small cell lung cancer cells,[56] and prevents myeloid cell. but not erythroid cell proliferation.[57] In contrast, epidermal and corneal-specific ablation of Notch1 led to hyperplasia and tumor formation in mice,[58] and a tumor suppressive role for activated Notch signaling has also been suggested in the prostate, lung, brain and liver.[34] Over-expression of a constitutively active form of Notch4 in a human adenocarcinoma cell line produced highly aggressive tumors in nude mice in comparison to cells expressing the intracellular domain of Notch2, which displayed tumor suppressor activity.[59] The subsequent activation of downstream effectors resulting from differential Notch/ligand interactions may also reflect tumor phenotype as the expression of Hes1, Hes3, Hey1, and Hey2 have been associated with several neoplasias including metastatic tumors.[60] Since we found differences in the relative expression of the tumors as well as the effectors, it is possible that the phenotypic differences observed within these tumors are directly attributable to the unique balances in specific receptor-mediated signals generated within the transfectants. However, it is important to note that while members of the Hes/Hey family are well characterized as Notch targets, there is evidence for Notch-independent activation of these genes. Pathways including c-jun N-terminal protein kinase[61] and BMP signaling[62] also regulate Hes/Hey activation, suggesting multiple stimuli within a tumor environment may impact the expression of these factors.

The differences in vessel network and necrosis we observe in the present study may also be attributable to the subtle changes in Notch signaling mediated by the primary activating ligands. Notch signaling from tumor cells have been shown to trigger Notch activation of neighboring EC's and consequently promote tumor angiogenesis.[63,64] Increased Dll4 has been associated with increased vasculature in human breast and kidney carcinomas in mice xenografts while reduction of Dll1 in endothelial cells by siRNA leads to inhibition of cellular functions.[65] Our results correlate to these finding in that Notch activation by Dll1 overexpression in the tumor cells leads to increased vessel development. Although Notch activation by Dll1 (our study) and Jag1[63] are pro-angiogenic, suppression of Notch signaling by their respective soluble ligands is not complementary. While sDl1 tumors displayed decreased tumor vessel development, the vessels formed by sJag1 transfectants were larger and more developed than those in sDl1 or control allographs. This pro-angiogenic behavior of the sJag1 ligand is in agreement with our *in vitro* and *in vivo* studies on these cells in which sJag1 promotes FGFR signaling and induces a cord-like phenotype in NIH3T3 fibroblasts grown and culture and produces large, dilated vessels in chick chorioallantoic assays.[33,35] These differential effects of ligand expression on tumor angiogenesis are likely the result of Notch/ligand regulation of angiogenic growth factors including VEGF, which was found to be highest in sJag1 and Dl1 samples.

Finally, our finding that the sJag1 and sDl1 transfectants developed into tumors internally populated by adipocyte or adipocyte-like cells was intriguing due to the reports that Notch signaling regulates adipogenesis[66–69] and NIH3T3 cells can differentiate into adipocytes under certain conditions.[70] The regulation of adipogenesis by Notch is complex and several studies support a bimodal signaling mechanism in which canonical Notch pathways must first be activated and then repressed during the early and late stages, respectively, of adipocyte differen-

tiation. At this time we cannot determine whether the adipocyte-like cells in either tumor types were the result of *in situ* differentiation of our NIH3T3 transfectants or due to the recruitment of endogenous pre-adipocytes to the tissue. In either case, the selective suppression of endogenous Notch signaling through either sDl1 or sJag1 appears to promote full or partial adipogenesis in these tumors. Intriguingly, the morphology of the lipid-accumulating cells within each tumor type was distinct with the sDl1 and sJag1 tumors containing adipocytes that were more similar to those found within white, adipose tissue white or brown respectively. The finding that both of these tumor types expressed higher levels of FAS than control or Dl1 tumors may be significant since the prognosis of several cancers, in particular breast cancer, is more severe in tumors expressing higher FAS activity.[71,72] Further exploration into the mechanism by which specific forms of the soluble ligands regulate adipogenesis and/or adipocyte gene expression in solid tumors may increase our understanding of the pathogenesis of cancers that rely extensively on fatty acids as an energy source.

In summary, Notch suppression has the effect of increasing the tumorigenicity of NIH3T3 cells *in vivo*, although this corresponds to different phenotypes of the resultant tumors. Conversely, our findings that activation of Notch signaling by Jag1 has a strong tumor suppressive phenotype, whereas Dl1 does not share this activity supports differential functions of these ligands in cellular transformation and tumor development. Further studies on ligand function in neoplastic cell lines and tumor models may provide insight into the signaling attributes of specific ligand/receptor interactions. In particular, the connection between ligand activity and the induction of specific Notch effectors (Hes/Hey) may be of importance since we found that relative expression of these transcriptional regulators differed significantly among tumor types. Since all vertebrate cells examined to date express some complement of Notch ligands and receptors and Notch signaling is required for homeostasis in mature cells and tissues, the development of therapeutic agents that can target specific receptor/ligand interactions may provide effective cancer treatments with reduced deleterious side effects.

Acknowledgments

We thank our Pathology Core (K. Carrier and V. Lindner) and MRI facility (M. Preda), which are supported by a grant from the National Center for Research Resources P20RR1555 (R. Friesel); Ms. Shawna Fox (University of New Hampshire) for technical assistance with the qRT-PCR experiments; and for expertise and technology, Dr. Gary Smejkal and Pressure BioSciences, Inc., South Easton, MA.

References

1. Artavanis-Tsakonas S, Rand MD, Lake RJ: Notch signaling: cell fate control and signal integration in development. Science 1999, 284:770–776
2. Bray SJ: Notch signalling: a simple pathway becomes complex. Nat Rev Mol Cell Biol 2006, 7:678–689
3. Miele L: Notch signaling. Clin Cancer Res 2006, 12:1074–1079
4. Conlon RA, Reaume AG, Rossant J: Notch1 is required for the coordinate segmentation of somites. Development 1995, 121:1533–1545
5. Hu QD, Ang BT, Karsak M, Hu WP, Cui XY, Duka T, Takeda Y, Chia W, Sankar N, Ng YK, Ling EA, Maciag T, Small D, Trifonova R, Kopan R, Okano H, Nakafuku M, Chiba S, Hirai H, Aster JC, Schachner M, Pallen CJ, Watanabe K, Xiao ZC: F3/contactin acts as a functional ligand for Notch during oligodendrocyte maturation. Cell 2003, 115:163–175
6. Jiang R, Lan Y, Chapman HD, Shawber C, Norton CR, Serreze DV, Weinmaster G, Gridley T: Defects in limb, craniofacial, and thymic development in Jagged2 mutant mice. Genes Dev 1998, 12:1046–1057
7. Joutel A, Corpechot C, Ducros A, Vahedi K, Chabriat H, Mouton P, Alamowitch S, Domenga V, Cecillion M, Marechal E, Maciazek J, Vayssiere C, Cruaud C, Cabanis EA, Ruchoux MM, Weissenbach J, Bach JF, Bousser MG, Tournier-Lasserve E: Notch3 mutations in CADASIL, a hereditary adult-onset condition causing stroke and dementia. Nature 1996, 383:707–710
8. Krebs LT, Xue Y, Norton CR, Sundberg JP, Beatus P, Lendahl U, Joutel A, Gridley T: Characterization of Notch3-deficient mice: normal embryonic development and absence of genetic interactions with a Notch1 mutation. Genesis 2003, 37:139–143
9. Li L, Krantz ID, Deng Y, Genin A, Banta AB, Collins CC, Qi M, Trask BJ, Kuo WL, Cochran J, Costa T, Pierpont ME, Rand EB, Piccoli DA, Hood L, Spinner NB: Alagille syndrome is caused by mutations in human Jagged1, which encodes a ligand for Notch1. Nat Genet 1997, 16:243–251
10. Lindner V, Booth C, Prudovsky I, Small D, Maciag T, Liaw L: Members of the Jagged/Notch gene families are expressed in injured arteries and regulate cell phenotype via alterations in cell matrix and cell-cell interaction. Am J Pathol 2001, 159:875–883
11. Oda T, Elkahloun AG, Pike BL, Okajima K, Krantz ID, Genin A, Piccoli DA, Meltzer PS, Spinner NB, Collins FS, Chandrasekharappa SC: Mutations in the human Jagged1 gene are responsible for Alagille syndrome. Nat Genet 1997, 16:235–242
12. Uyttendaele H, Marazzi G, Wu G, Yan Q, Sassoon D, Kitajewski J: Notch4/int-3, a mammary proto-oncogene, is an endothelial cell-specific mammalian Notch gene. Development 1996, 122:2251–2259
13. Xue Y, Gao X, Lindsell CE, Norton CR, Chang B, Hicks C, Gendron-Maguire M, Rand EB, Weinmaster G, Gridley T: Embryonic lethality and vascular defects in mice lacking the Notch ligand Jagged1. Hum Mol Genet 1999, 8:723–730
14. Zagouras P, Stifani S, Blaumueller CM, Carcangiu ML, Artavanis-Tsakonas S: Alterations in Notch signaling in neoplastic lesions of the human cervix. Proc Natl Acad Sci USA 1995, 92:6414–6418
15. Panin VM, Papayannopoulos V, Wilson R, Irvine KD: Fringe modulates Notch-ligand interactions. Nature 1997, 387:908–912
16. Trifonova R, Small D, Kacer D, Kovalenko D, Kolev V, Mandinova A, Soldi R, Liaw L, Prudovsky I, Maciag T: The non-transmembrane form of Delta1, but not of Jagged1, induces normal migratory behavior accompanied by fibroblast growth factor receptor 1-dependent transformation. J Biol Chem 2004, 279:13285–13288
17. Adam J, Myat A, Le Roux I, Eddison M, Henrique D, Ish-Horowicz D, Lewis J: Cell fate choices and the expression of Notch. Delta and Serrate homologues in the chick inner ear: parallels with Drosophila sense-organ development, Development 1998, 125:4645–4654
18. Kopan R, Schroeter EH, Weintraub H, Nye JS: Signal transduction by activated mNotch: importance of proteolytic processing and its regulation by the extracellular domain, Proc Natl Acad Sci USA 1996, 93:1683–1688
19. Ray WJ, Yao M, Mumm J, Schroeter EH, Saftig P, Wolfe M, Selkoe DJ, Kopan R, Goate AM: Cell surface presenilin-1 participates in the gamma-secretase-like proteolysis of Notch. J Biol Chem 1999, 274:36801–36807
20. Saxena MT, Schroeter EH, Mumm JS, Kopan R: Murine notch homologs (N1-4) undergo presenilin-dependent proteolysis. J Biol Chem 2001, 276:40268–40273
21. Hsieh JJ, Henkel T, Salmon P, Robey E, Peterson MG, Hayward SD: Truncated mammalian Notch1 activates CBF1/RBPJk-repressed genes by a mechanism resembling that of Epstein-Barr virus EBNA2. Mol Cell Biol 1996, 16:952–959
22. Jarriault S, Brou C, Logeat F, Schroeter EH, Kopan R, Israel A:

Signalling downstream of activated mammalian Notch. Nature 1995, 377:355–358
23. Kao HY, Ordentlich P, Koyano-Nakagawa N, Tang Z, Downes M, Kintner CR, Evans RM, Kadesch T: A histone deacetylase corepressor complex regulates the Notch signal transduction pathway. Genes Dev 1998, 12:2269–2277
24. Iso T, Kedes L, Hamamori Y: HES and HERP families: multiple effectors of the Notch signaling pathway. J Cell Physiol 2003, 194:237–255
25. Nakagawa O, Nakagawa M, Richardson JA, Olson EN, Srivastava D: HRT1. HRT2, and HRT3: a new subclass of bHLH transcription factors marking specific cardiac, somitic, and pharyngeal arch segments. Dev Biol 1999, 216:72–84
26. Axelson H: The Notch signaling cascade in neuroblastoma: role of the basic helix-loop-helix proteins HASH-1 and HES-1. Cancer Lett 2004, 204:171–178
27. Schweisguth F: Regulation of notch signaling activity. Curr Biol 2004, 14:R129–R138
28. Le Borgne R, Remaud S, Hamel S, Schweisguth F: Two distinct E3 ubiquitin ligases have complementary functions in the regulation of delta and serrate signaling in Drosophila. PLoS Biol 2005, 3:e96
29. Ascano JM, Beverly LJ, Capobianco AJ: The C-terminal PDZ-ligand of JAGGED1 is essential for cellular transformation. J Biol Chem 2003, 278:8771–8779
30. Bland CE, Kimberly P, Rand MD: Notch-induced proteolysis and nuclear localization of the Delta ligand. J Biol Chem 2003, 278:13607–13610
31. Kolev V, Kacer D, Trifonova R, Small D, Duarte M, Soldi R, Graziani I, Sideleva O, Larman B, Maciag T, Prudovsky I: The intracellular domain of Notch ligand Delta1 induces cell growth arrest. FEBS Lett 2005, 579:5798–5802
32. Small D, Kovalenko D, Kacer D, Liaw L, Landriscina M, Di Serio C, Prudovsky I, Maciag T: Soluble Jagged 1 represses the function of its transmembrane form to induce the formation of the Src-dependent chord-like phenotype. J Biol Chem 2001, 276:32022–32030
33. Small D, Kovalenko D, Soldi R, Mandinova A, Kolev V, Trifonova R, Bagala C, Kacer D, Battelli C, Liaw L, Prudovsky I, Maciag T: Notch activation suppresses fibroblast growth factor-dependent cellular transformation. J Biol Chem 2003, 278:16405–16413
34. Leong KG, Karsan A: Recent insights into the role of Notch signaling in tumorigenesis. Blood 2006, 107:2223–2233
35. Wong MK, Prudovsky I, Vary C, Booth C, Liaw L, Mousa S, Small D, Maciag T: A non-transmembrane form of Jagged-1 regulates the formation of matrix-dependent chord-like structures. Biochem Biophys Res Commun 2000, 268:853–859
36. Wong MK, Prudovsky I, Vary C, Booth C, Liaw L, Mousa S, Small D, Maciag T: A non-transmembrane form of Jagged-1 regulates the formation of matrix-dependent chord-like structures. Biochem Biophys Res Commun 2000 Feb 24, 268:853–859
37. Urs S, Harrington A, Liaw L, Small D: Selective expression of an aP2/Fatty Acid Binding Protein4-Cre transgene in non-adipogenic tissues during embryonic development. Transgenic Res 2006, 15:647–653
38. Smejkal GB, Witzmann FA, Ringham H, Small D, Chase SF, Behnke J, Ting E: Sample preparation for two-dimensional gel electrophoresis using pressure cycling technology. Anal Biochem 2007, 363:309–311
39. Hicks C, Ladi E, Lindsell C, Hsieh JJ, Hayward SD, Collazo A, Weinmaster G: A secreted Delta1-Fc fusion protein functions both as an activator and inhibitor of Notch1 signaling. J Neurosci Res 2002, 68:655–667
40. Jensen RL, Leppla D, Rokosz N, Wurster RD: Matrigel augments xenograft transplantation of meningioma cells into athymic mice. Neurosurgery 1998, 42:130–135; discussion 135–136
41. Iso T, Hamamori Y, Kedes L: Notch signaling in vascular development. Arterioscler Thromb Vasc Biol 2003, 23:543–553
42. Karsan A: The role of notch in modeling and maintaining the vasculature. Can J Physiol Pharmacol 2005, 83:14–23
43. Holmes DI, Zachary I: The vascular endothelial growth factor (VEGF) family: angiogenic factors in health and disease. Genome Biol 2005, 6:209
44. Yancopoulos GD, Davis S, Gale NW, Rudge JS, Wiegand SJ, Holash J: Vascular-specific growth factors and blood vessel formation. Nature 2000, 407:242–248
45. Fromm C, Coso OA, Montaner S, Xu N, Gutkind JS: The small GTP-binding protein Rho links G protein-coupled receptors and Galpha12 to the serum response element and to cellular transformation. Proc Natl Acad Sci USA 1997, 94:10098–10103
46. Schuebel KE, Bustelo XR, Nielsen DA, Song BJ, Barbacid M, Goldman D, Lee IJ: Isolation and characterization of murine vav2, a member of the vav family of proto-oncogenes. Oncogene 1996, 13:363–371
47. Radtke F, Raj K: The role of Notch in tumorigenesis: oncogene or tumour suppressor?. Nat Rev Cancer 2003, 3:756–767
48. Weng AP, Aster JC: Multiple niches for Notch in cancer: context is everything. Curr Opin Genet Dev 2004, 14:48–54
49. Zhang N, Gridley T: Defects in somite formation in lunatic fringe-deficient mice. Nature 1998, 394:374–377
50. Brooker R, Hozumi K, Lewis J: Notch ligands with contrasting functions: jagged1 and Delta1 in the mouse inner ear. Development 2006, 133:1277–1286
51. Neves H, Weerkamp F, Gomes AC, Naber BA, Gameiro P, Becker JD, Lucio P, Clode N, van Dongen JJ, Staal FJ, Parreira L: Effects of Delta1 and Jagged1 on early human hematopoiesis: correlation with expression of notch signaling-related genes in CD34+ cells. Stem Cells 2006, 24:1328–1337
52. Lehar SM, Dooley J, Farr AG, Bevan MJ: Notch ligands Delta 1 and Jagged1 transmit distinct signals to T-cell precursors. Blood 2005, 105:1440–1447
53. Tohda S, Kogoshi H, Murakami N, Sakano S, Nara N: Diverse effects of the Notch ligands Jagged1 and Delta1 on the growth and differentiation of primary acute myeloblastic leukemia cells. Exp Hematol 2005, 33:558–563
54. Wilson A, Radtke F: Multiple functions of Notch signaling in self-renewing organs and cancer. FEBS Lett 2006, 580:2860–2868
55. Morimura T, Miyatani S, Kitamura D, Goitsuka R: Notch signaling suppresses IgH gene expression in chicken B cells: implication in spatially restricted expression of Serrate2/Notch1 in the bursa of Fabricius. J Immunol 2001, 166:3277–3283
56. Sriuranpong V, Borges MW, Ravi RK, Arnold DR, Nelkin BD, Baylin SB, Ball DW: Notch signaling induces cell cycle arrest in small cell lung cancer cells. Cancer Res 2001, 61:3200–3205
57. Walker L, Lynch M, Silverman S, Fraser J, Boulter J, Weinmaster G, Gasson JC: The Notch/Jagged pathway inhibits proliferation of human hematopoietic progenitors in vitro. Stem Cells 1999, 17:162–171
58. Nicolas M, Wolfer A, Raj K, Kummer JA, Mill P, van Noort M, Hui CC, Clevers H, Dotto GP, Radtke F: Notch1 functions as a tumor suppressor in mouse skin. Nat Genet 2003, 33:416–421
59. O'Neill CF, Urs S, Cinelli C, Lincoln A, Nadeau RJ, Leon R, Toher J, Mouta-Bellum C, Friesel RE, Liaw L: Notch2 signaling induces apoptosis and inhibits human MDA-MB-231 xenograft growth. Am J Pathol 2007, 171:1023–1036
60. Zavadil J, Cermak L, Soto-Nieves N, Bottinger EP: Integration of TGF-beta/Smad and Jagged1/Notch signalling in epithelial-to-mesenchymal transition. EMBO J 2004, 23:1155–1165
61. Curry CL, Reed LL, Nickoloff BJ, Miele L, Foreman KE: Notch-independent regulation of Hes-1 expression by c-Jun N-terminal kinase signaling in human endothelial cells. Lab Invest 2006, 86:842–852
62. Takizawa T, Ochiai W, Nakashima K, Taga T: Enhanced gene activation by Notch and BMP signaling cross-talk. Nucleic Acids Res 2003, 31:5723–5731
63. Zeng Q, Li S, Chepeha DB, Giordano TJ, Li J, Zhang H, Polverini PJ, Nor J, Kitajewski J, Wang CY: Crosstalk between tumor and endothelial cells promotes tumor angiogenesis by MAPK activation of Notch signaling. Cancer Cell 2005, 8:13–23
64. Rehman AO, Wang CY: Notch signaling in the regulation of tumor angiogenesis. Trends Cell Biol 2006, 16:293–300
65. Patel NS, Li JL, Generali D, Poulsom R, Cranston DW, Harris AL: Up-regulation of delta-like 4 ligand in human tumor vasculature and the role of basal expression in endothelial cell function. Cancer Res 2005, 65:8690–8697
66. Ross DA, Hannenhalli S, Tobias JW, Cooch N, Shiekhattar R, Kadesch T: Functional analysis of Hes-1 in preadipocytes. Mol Endocrinol 2006, 20:698–705
67. Nueda ML, Baladron V, Sanchez-Solana B, Ballesteros MA, Laborda J: The EGF-like protein dlk1 inhibits notch signaling and potentiates adipogenesis of mesenchymal cells. J Mol Biol 2007, 367:1281–1293

68. Garces C, Ruiz-Hidalgo MJ, Font de Mora J, Park C, Miele L, Goldstein J, Bonvini E, Porras A, Laborda J: Notch-1 controls the expression of fatty acid-activated transcription factors and is required for adipogenesis. J Biol Chem 1997, 272:29729–29734
69. Ross DA, Rao PK, Kadesch T: Dual roles for the Notch target gene Hes-1 in the differentiation of 3T3-L1 preadipocytes. Mol Cell Biol 2004, 24:3505–3513
70. Zuo X, Li G, Luo T, Li J, Liu Y, Luo M: Differentiation of NIH3T3 fibroblasts into adipocytes induced by peroxisome proliferator activated receptor gamma 2 expression. Chin Med J (Engl) 2001, 114:916–920
71. Hunt DA, Lane HM, Zygmont ME, Dervan PA, Hennigar RA: MRNA stability and overexpression of fatty acid synthase in human breast cancer cell lines. Anticancer Res 2007, 27:27–34
72. Hennigar RA, Pochet M, Hunt DA, Lukacher AE, Venema VJ, Seal E, Marrero MB: Characterization of fatty acid synthase in cell lines derived from experimental mammary tumors. Biochim Biophys Acta 1998, 1392:85–100